Article

Changes in Runoff in the Source Region of the Yellow River Basin Based on CMIP6 Data under the Goal of Carbon Neutrality

Yihua Liu [1,2], Lyuliu Liu [3,*], Lin Li [2,4], Hongmei Li [2,5], Hongmei Xu [3], Jing Yang [6], Shiyin Tao [1] and Baowen Zhu [7]

[1] Climate Center of Qinghai, Xining 810001, China; yihualiu12@sina.cn (Y.L.); qhzxshiyintao@163.com (S.T.)
[2] Key Laboratory of Disaster Prevention and Mitigation of Qinghai Province, Xining 810001, China; lhm761026@tom.com (H.L.)
[3] National Climate Center, China Meteorological Administration, Beijing 100081, China
[4] Qinghai Meteorological Bureau, Xining 810001, China
[5] China Global Atmosphere Watch Baseline Observatory, Xining 810001, China
[6] Gang Cha Meteorological Bureau, Qinghai 812300, China; 13897309035@163.com
[7] Qinghai Meteorological Administration Training Center, Xining 810001, China; mszzbw@163.com
[*] Correspondence: liull@cma.gov.cn

Abstract: China is committed to achieving carbon neutrality before 2060. This study projected the changes in climate and runoff in the source region of the Yellow River Basin for 2021–2060 under lower carbon emission pathways (SSP1–2.6 and SSP2–4.5) using a statistically downscaled climate dataset and the SWAT hydrological model. Results showed that the climate will become warmer and wetter from 2021–2060. In comparison with the baseline period (1995–2014), in terms of the ensemble mean, annual mean air temperature, annual precipitation, and annual runoff will increase by 1.3 °C and 1.6 °C, by 11.1% and 11.2%, and by 12.8% and 11.9% under SSP1–2.6 and SSP2–4.5 scenarios, respectively. Moreover, the seasonal pattern of runoff was projected to change. The proportion of monthly runoff to the annual total will decrease by 0.6–1.0% in summer but increase by 0.1–1.0% during the period from January to April and September to December. The multimodel ensemble mean (MEM) of extremely high monthly flow (Q10) will increase by 3.5–13.4% in the flood season (June to August) and water storage season (September to December). The MEM of extremely low monthly flow (Q90) will increase by 19.4–26.2% from February to April but decrease by 5.0–8.9% in January, May, and December. Thus, the warmer and wetter climate from 2021–2060 will likely cause flatter seasonal distribution of runoff, lower risk of water scarcity at the annual scale and of drought from February to April, but higher risk both of flood in the flood season and of drought in December, January, and May. Generally, the flatter pattern of runoff would likely alleviate water scarcity in the dry and water storage seasons to some degree, and the increase in monthly runoff in the water storage season will benefit hydroelectric power generation and agriculture and animal husbandry production. However, in some years, the increase in Q10 in the flood season will likely increase flood prevention pressure, and the decrease in Q90 in May will likely obstruct grass revival.

Keywords: climate change impact; runoff projection; Yellow River; SWAT model; CMIP6 models; carbon neutrality

1. Introduction

Water resources are of great importance to achieve the goal of carbon neutrality. Hydropower can reduce fossil fuel consumption by supplying renewable energy in conjunction with wind and solar power. Water resources are also required for the green transformation of the urban energy and industrial structure. Global warming has accelerated the circulation of water vapor, which led to an increase in evaporation and the change in the spatiotemporal distribution of both precipitation and runoff [1,2]. Alteration of the distribution of both precipitation and discharge has produced more frequent and stronger extreme

hydrometeorological events [3,4], that have impacts on ecosystems [5]. The Yellow River is the second-largest river in China in terms of length. It supports 30.3% of the national population and possesses 2.6% of the national total water resources [6]. The source region of the Yellow River is upstream of the Tangnaihai hydrological gauging station. It covers 15% of the entire area of the Yellow River Basin and generates 35% of basin runoff [7]. The ecosystem in the region is fragile and sensitive to changes in climate and runoff. Recently, in the source region, extreme hydrological events such as rainstorms and floods have become more frequent, but annual runoff has diminished [8–12]. For example, summer precipitation broke the historical maximum value in Guoluo State in Qinghai Province in 2020 and caused flooding along the Yellow River. To prevent and control such flooding, the Longyangxia Reservoir operated for more than 40 days beyond the flood level. Thus, it is of great importance to project the changes in runoff and extreme hydrological events under global warming for both water resource security in the source region and in the entire basin of the Yellow River and achieving the goal of carbon neutrality.

A global climate model (GCM) is an important tool for predicting climate change [13]. The Coupled Model Intercomparison Project Phase 5 (CMIP5) projected a warming climate in the source region of the Yellow River for 2020–2059 [14]. The newly released GCMs of the Coupled Model Intercomparison Project Phase 6 (CMIP6) have been improved further. They can better reproduce the spatial patterns of climatic elements and produce smaller deviations of climatic simulations in comparison with those of CMIP5 [15,16]. Based on CMIP6 GCMs, a wetter climate for 2021–2100 under common shared socioeconomic pathway (SSP) and representative concentration pathway (SSP–RCP) scenarios (i.e., SSP1–26, SSP2–45, SSP3–70, and SSP5–85 [17]) and increasing trend of annual runoff for 2021–2100 under SSP1–26 and SSP2–45 scenarios but decreasing trend of annual runoff for 2061–2100 under the SSP5–85 scenario were projected in the region [18]. Projected change amplitudes and even change directions of climate and runoff in the future may be different due to uncertainties from emission scenarios, climate forcing, and hydrological models. Therefore, it is necessary to enrich the investigation on the changes in climate and hydrological variables using the newly released CMIP6 GCMs for climate forcing.

The primary aim of this study was to explore the variations in climate and the responses of runoff regarding the pathway to achieving the goal of carbon neutrality using the soil water assessment tool (SWAT) hydrological model and CMIP6 GCMs. Firstly, the performance of the SWAT model and the reproducibility of a downscaled dataset from CMIP6 GCMs was evaluated. Then, the changes in annual temperature and precipitation were projected for the period 2021–2060 under two "double carbon" pathways. Following them, the changes in annual runoff, monthly mean runoff, and extreme monthly runoff in the source region of the Yellow River Basin were explored in sequence. The results could support the safe operation of the Longyangxia Reservoir, rational water allocation, and development of hydro–wind–solar energy in the Yellow River Basin with the goal of achieving carbon neutrality.

2. Materials and Methodologies

2.1. Study Region

The Yellow River is the second largest river in terms of length in China. This study focused on its source region (32°12′–35°48′ N, 95°50′–103°28′ E) located upstream of the Tangnaihai hydrological gauging station. The area of the source region is approximately $13.0 \times 10^4 \text{ km}^2$, which accounts for 15% of the entire area of the Yellow River Basin. The elevation varies from 2678 to 6253 m. Owing to its unique geographical location, the Yellow River Basin serves as a regulator of the climate in China. The annual mean air temperature, annual mean minimum air temperature, and mean maximum air temperature varied from −3.7 to −1.1 °C, from −10.6 to −7.2 °C, and from 4.0 to 7.1 °C from 1961–2020, respectively. They have risen at the rate of 0.3, 0.5, and 0.3 °C/10a ($p < 0.001$), respectively. The annual mean precipitation varies from 357.0 to 677.6 mm in the study region, and it has increased with an overall rate of 8.8 mm/10a ($p < 0.1$). Since 2000, it has increased at

the rate of 54.8 mm/10a. Annual runoff is approximately 20.8×10^9 m^3, which accounts for approximately 35% of the total runoff in the Yellow River Basin. Floods occur mainly from July to October, reflecting the distribution of precipitation throughout the year and the extreme precipitation that occurs frequently during this period.

2.2. Dataset

In this study, spatial data of the Yellow River Basin, including digital elevation model (DEM), land use, and soil type, were obtained online (http://westdc.westgis.ac.cn/) (accessed on 5 July 2021). The resolution of the DEM was 1:250,000, and the spatial resolution of the land use data in 2005 was 1000 m. The soil data with 0.25° × 0.25° resolution were obtained from a harmonized world soil database by the Food and Agriculture Organization of the United Nations. These data were used in the setup of the SWAT hydrological model. Observed daily meteorological data with 0.25° × 0.25° resolution (Figure 1) from 1961 to 2016 were obtained from the CN05.1 dataset, which was developed using climate data observed at more than 2400 meteorological stations in China. First, the gridded climatology was interpolated with the thin plate smoothing splines method, and the gridded anomaly was derived with the angular distance weighing method. Then, the CN05.1 dataset was developed by adding the gridded climatology and the anomaly. This dataset has been used widely to assess the performance of climate models and to investigate the impact of climate change in China [19,20]. In this study, the meteorological data of daily precipitation and mean, maximum, and minimum air temperature from 1961 to 2014 were used to calibrate the SWAT hydrological model, Climate simulation datasets from eight GCM$_S$ (Table 1) for the period 1961–2014 for the historical experiment and for the period 2015–2100 under SSP1–2.6 and SSP2–4.5 were obtained from the National Climate Center [21]. They represented statistically downscaled results with spatial disaggregation and bias correction using an equal distance cumulative distribution function based on CMIP6 GCMs. The results reproduced the spatial patterns of annual precipitation, annual temperature, and extreme climatic events better than the raw simulations of the GCMs for the Yellow River Basin [22], irrespective of comparison with a single model or with the multimodel ensemble mean (MEM). The daily data of precipitation, maximum air temperature, and minimum air temperature were used to force the SWAT model to project the changes in runoff and extreme flow. This study used MEMs to represent the general projected changes in climate, runoff, and flooding. Monthly observed runoff through the Tangnaihai hydrological station from 1961–2020 were obtained from the Yellow River Resources Bureau. These data were used to calibrate and verify the SWAT hydrological model.
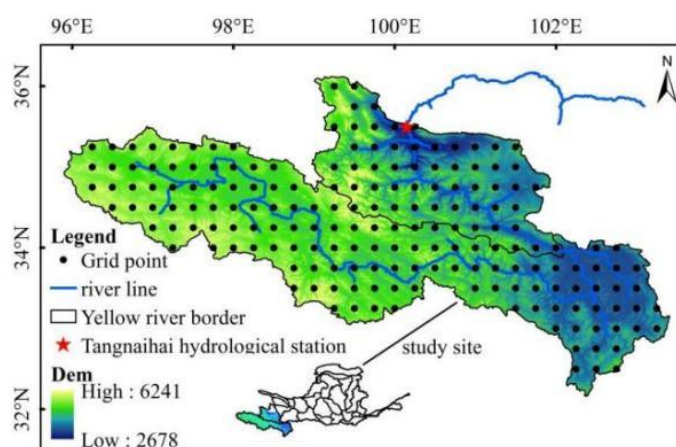
Figure 1. Location of the Yellow River Basin and topography of the source region of the Yellow River together with the grid of the downscaled climate datasets used in this study.

Table 1. General information of eight selected CMIP6 models.

ID	Name	Affiliated Country and Research Unit	Atmos. Lat/Lon Grid (°)
1	ACCESS–ESM–1–5 (ACESS)	Commonwealth Scientific and Industrial Research Organisation (Australia)	1.2° × 1.8°
2	BCC–CSM2–MR (BCC)	Beijing Climate Center, China Meteorological Administration (China)	1.1° × 1.1°
3	CCCma–CanESM5 (CCCma)	Canadian Centre for Climate Modelling and Analysis (Canada)	2.8° × 2.8°
4	CNRM–ESM2–1 (CNRM)	Centre National de Recherches Météorologiques, Centre Européen de Recherche et de Formation Avancée en Calcul Scientifique (France)	1.4° × 1.4°
5	HadGEM3–GC31–LL (HadGEM)	Met Office Hadley Centre (United Kingdom)	1.3° × 1.9°
6	IPSL–CM6A–LR (IPSL)	Institut Pierre Simon Laplace (France)	1.3° × 2.5°
7	MIROC6 (MIROC)	Japan Agency for Marine–Earth Science and Technology, Atmosphere and Ocean Research Institute (The University of Tokyo), National Institute for Environmental Studies, and RIKEN Center for Computational Science (Japan)	1.4° × 1.4°
8	MPI–ESM1–2–HR (MPI–ESM)	Max Planck Institute for Meteorology (Germany)	0.9° × 0.9°

2.3. Hydrological Model

In this study, the SWAT hydrological model was used to simulate runoff in the source region of the Yellow River. The SWAT model is a physically based, semi-distributed hydrological model developed by the United States Department of Agriculture Agricultural Research Service [23]. Based on a digital elevation model, a watershed can be divided into several subbasins, which can be further divided into hydrological response units based on land use, soil type, and slope. The water balance is calculated for each hydrological response unit, and the Soil Convention Service (SCS) runoff curve and the Penman–Monteith method are used to simulate the surface runoff and evapotranspiration processes. The SWAT model has been used to replicate processes such as surface runoff, groundwater, soil temperature, soil moisture, generation and transport of sand, nutrient loss, and other agricultural management processes [24–29].

The SWAT Calibration Uncertainty Program (SWAT–CUP) is a predefined program that links the procedures of SUFI–2, PSO, MCMC, GLUE, and Parasol to the SWAT model. This enables sensitivity analysis, calibration, validation, and uncertainty analysis of the SWAT model. In this study, SUFI–2 was used to identify sensitive parameters and to calibrate the SWAT model. We adopted the metrics of the coefficient of determination (R^2), Nash–Sutcliffe efficiency index (E_{ns}), and percentage bias ($PBIAS$) for the evaluation of model performance.

The metric of R^2 was used to assess the temporal correlation between the simulations and the observations. The R^2 value can range from 0 to 1 and as the value of R^2 becomes closer to 1, the model becomes more accurate. The metric of E_{ns} was used to assess the predictive power of the hydrological model. The E_{ns} value can range from $-\infty$ to 1. The prediction is worse than the observed mean if E_{ns} less than 0. The prediction is as accurate as the observed mean if the value is 0, and as the value of E_{ns} becomes closer to 1, the model becomes more accurate. $PBIAS$ was used to measure the average tendency of the simulation to be larger or smaller than the observation relative to the observation throughout the period assessed. The optimal value is 0, with low-magnitude values indicating accurate model simulation. Positive (negative) values indicate the overestimation (underestimation) bias of the model. Generally, if E_{ns} is greater than 0.50, R^2 is greater than 0.6, and $PBIAS$ is within ±25% for the calibration period (1961–1989) and the validation period (1990–2015), the

hydrological model is judged to be satisfactory and may be used to simulate runoff in the study area [30,31]. The formulas for the calculation of E_{ns}, R^2, and *PBIAS* are as follows:

$$E_{ns} = 1 - \frac{\sum_{i=1}^{n}(Q_{obs,i} - Q_{sim,i})^2}{\sum_{i=1}^{n}(Q_{obs,i} - \overline{Q_{obs}})^2} \tag{1}$$

$$R^2 = \frac{\left[\sum_{i=1}^{n}(Q_{obs,i} - \overline{Q_{obs}})(Q_{sim,i} - \overline{Q_{sim}})\right]^2}{\sum_{i=1}^{n}(Q_{obs,i} - \overline{Q_{obs}})^2 \sum_{i=1}^{n}(Q_{sim,i} - \overline{Q_{sim}})^2} \tag{2}$$

$$PBIAS = 100 \times \frac{\sum_{i=1}^{n}Q_{sim,i} - \sum_{i=1}^{n}Q_{obs,i}}{\sum_{i=1}^{n}Q_{obs,i}} \tag{3}$$

where Q_{obs} and Q_{sim} are the observed and the simulated monthly runoff, respectively, $\overline{Q_{obs}}$ and $\overline{Q_{sim}}$ are the mean of observed and simulated monthly runoff series, respectively, i is month, and n is the length of monthly runoff series during the calibration or validation period.

2.4. Reproducibility Assessment of Climate Dataset

The seasonal patterns of temperature and precipitation simulation by the downscaled dataset were compared with the observations for every month in terms of the MEM of the eight GCMs from 1961 to 2014, which included all the years of the downscaled dataset.

2.5. Runoff Projection

China is committed to the goal of achieving carbon neutrality by 2060. Here, climate change compared to the base period (1995–2014) was projected based on the downscaled climate from the eight CMIP6 GCMS for 2021–2060 under the SSP1–2.6 and SSP2–4.5 scenarios. Then, the changes in runoff were projected for the same period, the first half of the period (2021–2040), and the second half of the period (2041–2060) under the two scenarios. The projected metrics included annual mean temperature, annual precipitation, annual runoff, the percentage of monthly runoff to annual runoff, extreme monthly low flow (Q90), and extreme monthly high flow (Q10) [32,33]. The proportion of monthly runoff in the annual runoff is the percentage of monthly runoff to the annual total runoff. Q90 and Q10 represent the monthly flow exceeding 90% and 10% during the entire period investigated, respectively. The seasonal patterns of mean and extreme monthly runoff were further analyzed for the flood season (June to August), water storage season (September to November), and dry season (December to May), which are delimited according to the regulations for water resource management and reservoir regulation in the Yellow River Basin.

Droughts are the result of precipitation shortage over a long period, while floods are the result of excessive precipitation. When hydrological droughts happen, low monthly streamflow is usually observed, but when floods happen high monthly streamflow is usually observed. The changes in Q90 and Q10 were used to represent the changes in the risk of drought and flooding.

3. Results

3.1. Calibration and Validation of the SWAT Model

As listed in Table 2, E_{ns} was 0.76, R^2 was 0.86, and *PBIAS* was smaller than 10% for the periods of calibration and validation (Table 2). Thus, it was judged that the performance of the SWAT model is satisfactory in simulating monthly runoff through the Tangnaihai hydrological station according to the criteria adopted for the evaluation of the hydrological model. The seasonal pattern of the simulated runoff matches that of the observations during the two periods well, whereas the extremely high monthly flows were underestimated (Figure 2). To reduce the bias impact of the extremes to some degree, the changes in runoff

relative to the base period were explored using the calibrated SWAT model forced by the downscaled climate datasets of the eight CMIP6 GCMs.

Table 2. Evaluation of the SWAT model in terms of monthly runoff through the Tangnaihai hydrological station in the Yellow River Basin.

Station	Period	R^2	E_{ns}	PBIAS (%)
Tangnaihai	Calibration (1961–1989)	0.86	0.76	6.2
	Verification (1990–2015)	0.86	0.76	6.3
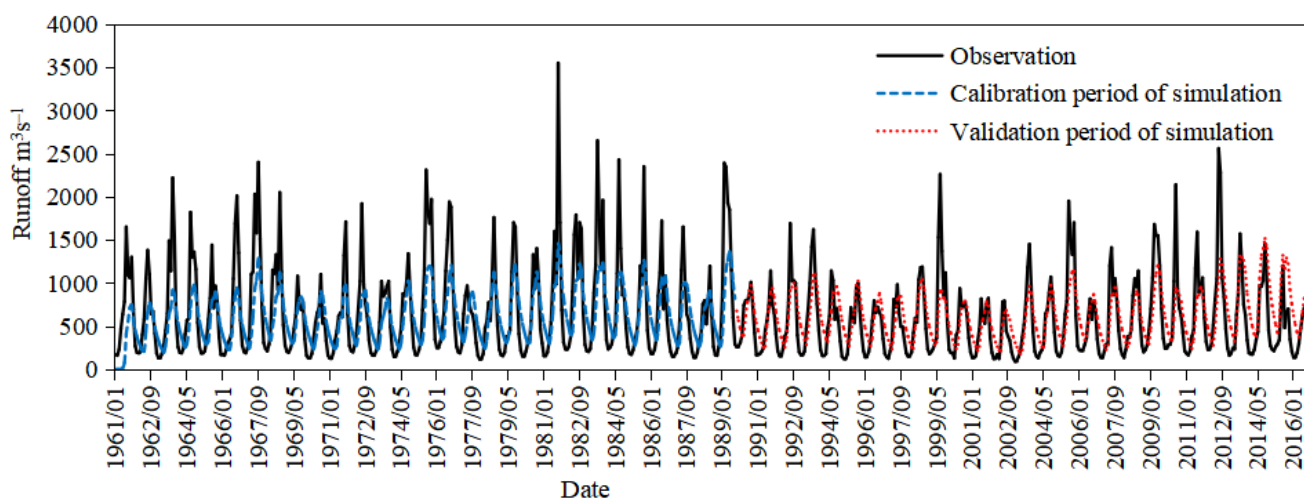
Figure 2. Observed and simulated monthly runoff through the Tangnaihai hydrological station in the source region of the Yellow River Basin.

3.2. Reproducibility Assessment of Climate Dataset

The MEMs of the eight CMIP6 GCMs were compared with the observations to assess the simulation performance of the downscaled dataset. The observations showed that the average annual air temperature in the source region of the Yellow River Basin from 1961–2014 was approximately −2.6 °C and that it rose at the rate of 0.35 °C/10a ($p < 0.05$). The average annual precipitation was 540.7 mm, and it increased at the rate of 8.8 mm/10a ($p < 0.01$). The warming and wetting trend in the source region of the Yellow River Basin is obvious. The MEMs of the downscaled data reproduced the warmer and wetter trends from 1961–2014 but simulated a cold bias of −0.2 °C and a wet bias of 3%. Additionally, the downscaled dataset reproduced the seasonal pattern of both temperature and precipitation (Figure 3). Similar to the observations, the simulated monthly temperature was high and the simulated precipitation was abundant in the rainy season (May to September) but the temperature was lower and the largest amount of precipitation was smaller in other months. The peak temperature and the largest amount of precipitation observed in July were also well reproduced. Thus, it was considered that the ensemble mean of the downscaled dataset is suitable for simulating both precipitation and temperature in the study region and for projecting runoff change by forcing the SWAT hydrological model for the study area.

3.3. Changes in Climatic Variables

Figure 4 illustrates the warming and wetting trends from 2021–2060 under the SSP1–2.6 and SSP2–4.5 scenarios in the source region of the Yellow River (Figure 4). The MEM annual air temperature was projected to rise at the rate of 0.2 and 0.3 °C/10a under the SSP1–2.6 and SSP2–4.5 scenarios, respectively. The multiyear mean annual air temperature was expected to rise by 1.1 and 1.2 °C for the first half of the period, by 1.5 and 1.9 °C for

the second half of the period, and by 1.3 and 1.6 °C for 2021–2060 under the SSP1–2.6 and SSP2–4.5 scenarios, respectively (Figure 5a). Spatially, the MEM annual temperature was projected to rise faster in the southeast of the study region than in the northwest (Figure 6a,b). However, the magnitude of the mean rise will be different among the eight GCMs for 2021–2060. The annual temperature was projected to rise fastest by the CCCma model under the SSP1–2.6 scenario but to rise slowest by the BCC and MPI–ESM models under the SSP1–2.6 scenario and by the MPI–ESM model under the SSP2–4.5 scenario. The largest and smallest magnitude of the projected rise in annual air temperature will be 2.2 and 0.8 °C, respectively.
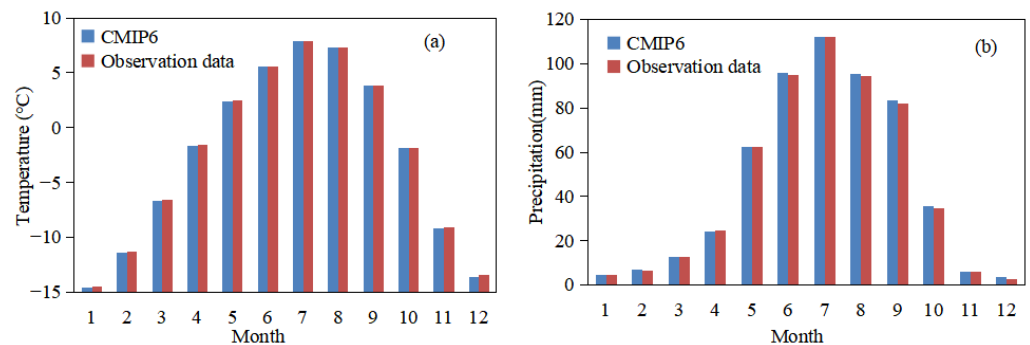
Figure 3. Comparison of monthly (**a**) temperature and (**b**) precipitation between the CMIP6 MEM and the observations from 1961–2014.
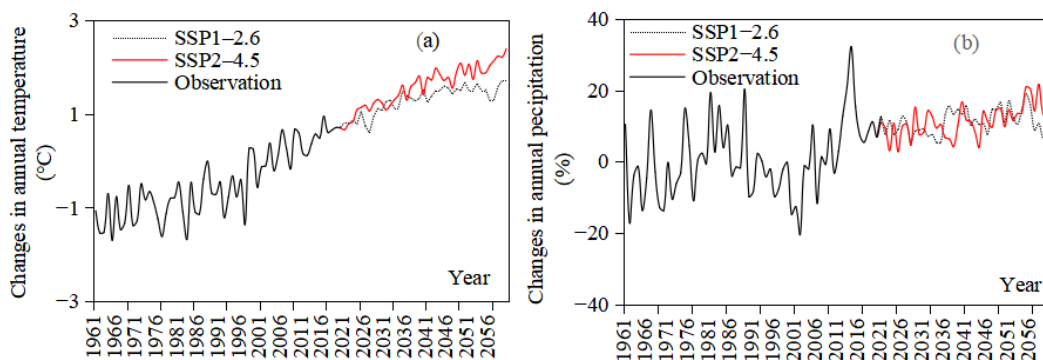
Figure 4. Changes in ensemble mean of annual mean temperature (**a**) and annual precipitation (**b**) in the source region of Yellow River for 1961–2060 relative to 1995–2014 under the SSP1–2.6 and SSP2–4.5 scenarios.
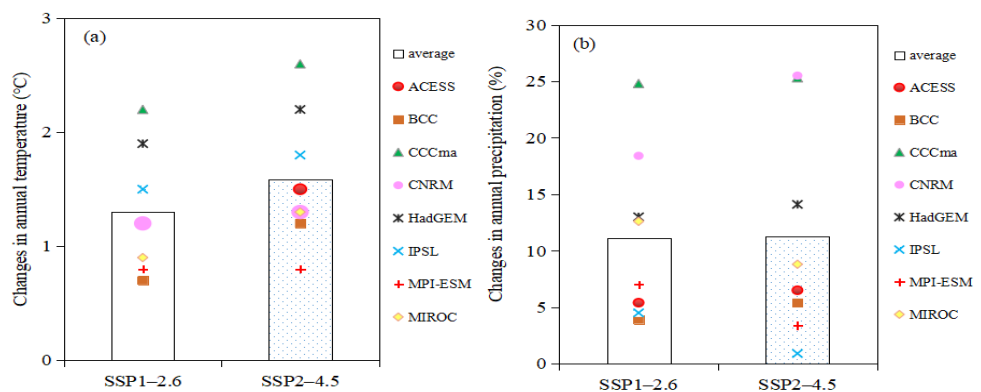
Figure 5. Projected changes in ensemble annual (**a**) air temperature and (**b**) precipitation in the source region of the Yellow River Basin for 2021–2060 relative to 1995–2014 under the SSP1–2.6 and SSP2–4.5 scenarios.
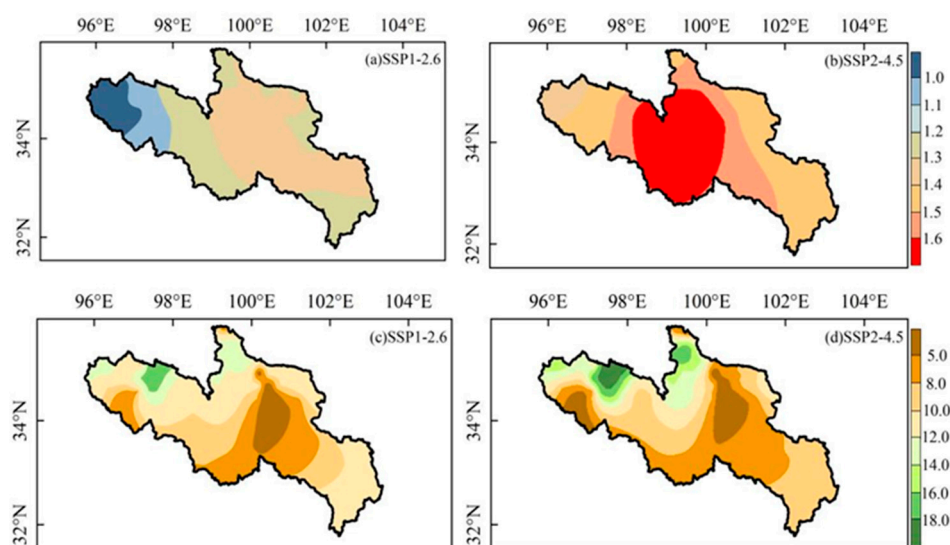
Figure 6. The spatial distribution of change in ensemble annual (**a**,**b**) air temperature (unit: °C) and (**c**,**d**) precipitation (unit: %) in the source region of the Yellow River Basin from 2021–2060 under two scenarios.

Annual precipitation was projected to increase at the rate of 6.0 and 12.0 mm/10a from 2021–2060 under the SSP1–2.6 scenario and the SSP2–4.5 scenario, respectively. The multiyear mean annual precipitation was projected to increase by 9.9% (SSP1–2.6 scenario) and 9.2% (SSP2–4.5 scenario) for the first half of the period (2021–2040), by 12.5% (SSP1–2.6 scenario) and 13.3% (SSP2–4.5 scenario) for the second half of the period (2041–2060), and by 11.1% and 11.2% for 2021–2060 under the SSP1–2.6 scenario and the SSP2–4.5 scenario, respectively (Figure 5b). Spatially, the MEM of the annual precipitation will increase by less than 15.0% in central and southeastern parts of the study area, while it will decrease by more than 15.0% in the northwest from 2021–2060 (Figure 6c,d). Moreover, uncertainties in the changes in precipitation associated with the GCMs and the SSP–RCP scenarios were projected (Figure 4b). Under the two scenarios, the multiyear mean annual precipitation will increase fastest by the CCCma and CNRM models, i.e., at a rate of 18.4–25.5%, but it was projected to increase by less than 15.0% by the other GCMs.

3.4. Variation of Annual Runoff

Figure 7 shows the variations in multiyear mean and decadal mean annual runoff for 2021–2060 under the two lower scenarios. The MEM multiyear mean annual runoff for 2021–2060 was expected to increase by 12.8% and 11.9% under the SSP1–2.6 scenario and the SSP2–4.5 scenario, respectively (Figure 7a). It was projected to increase by most GCMs, especially the CCCma, CNRM, and HadGEM models, but it was projected to decrease by the IPSL model (Figure 7b). The decadal mean was projected to fluctuate from the 2020s to the 2050s. It was projected to decrease by the IPSL and BCC models from the 2020s to the 2050s under both scenarios and by the IPSL model from 2051–2060 under the SSP2–4.5 scenario, whereas it was projected to increase by the ACESS, CCCma, CNRM, HadGEM, MPI–ESM, and MIROC models under both scenarios. The MEM decadal mean runoff was projected to increase by 15.2% and 14.1% in the 2040s and the 2050s, respectively, under the SSP1–2.6 scenario, whereas it was projected to increase by only 10.1–11.5% in other decades. In each decade from the 2020s to the 2050s, it was projected to increase by 9.9%, 10.9%, 11.9%, and 12.9%, respectively, under the scenario of SSP2–4.5. Overall, against the background of global warming, simulated runoff shows a varying trend of increase under the two SSP scenarios, and the degree of increase in runoff was expected to be greater under the low SSP scenario than under the high SSP scenario.
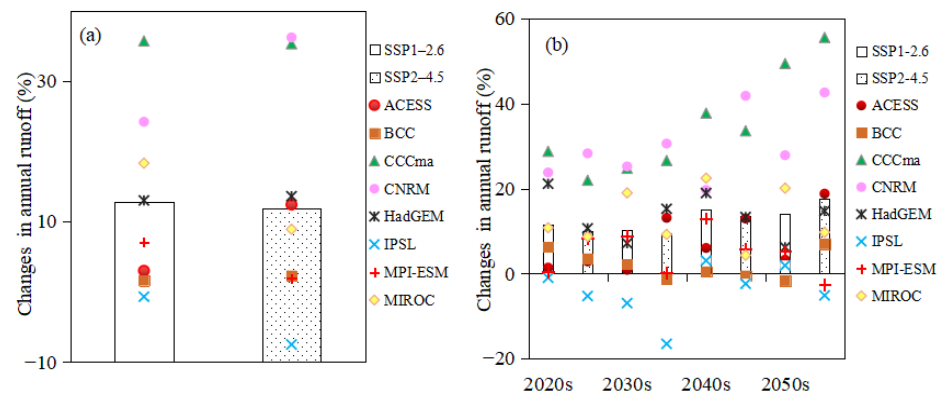
Figure 7. Expected changes in ensemble mean (**a**) annual runoff for 2021–2060 and (**b**) decadal mean annual runoff relative to 1995–2014 in the source region of Yellow River under the two scenarios.

3.5. Variation in Monthly Runoff

Figure 8 shows the changes in monthly runoff for 2021–2060 and for the first and second half of the period under the SSP1–2.6 and SSP2–4.5 scenarios. The MEM monthly runoff was projected to be larger than the baseline runoff in all months in both halves of the period. The MEM monthly runoff was expected to increase faster in the second half of the period than in the first half of the period, i.e., an increase of 14.6% and 11.0%, respectively. Large uncertainties are also evident among the 12 months and the eight GCMs. The MEM runoff was projected to increase by 46.4–93.8% in March and April, but by only 3.9–15.2% during the period from May to September. Moreover, runoff was projected to decrease by 1.7–15.5% by the ACESS, BCC, IPSL, and MPI–ESM models during the period from May to July but projected to increase by the other models.
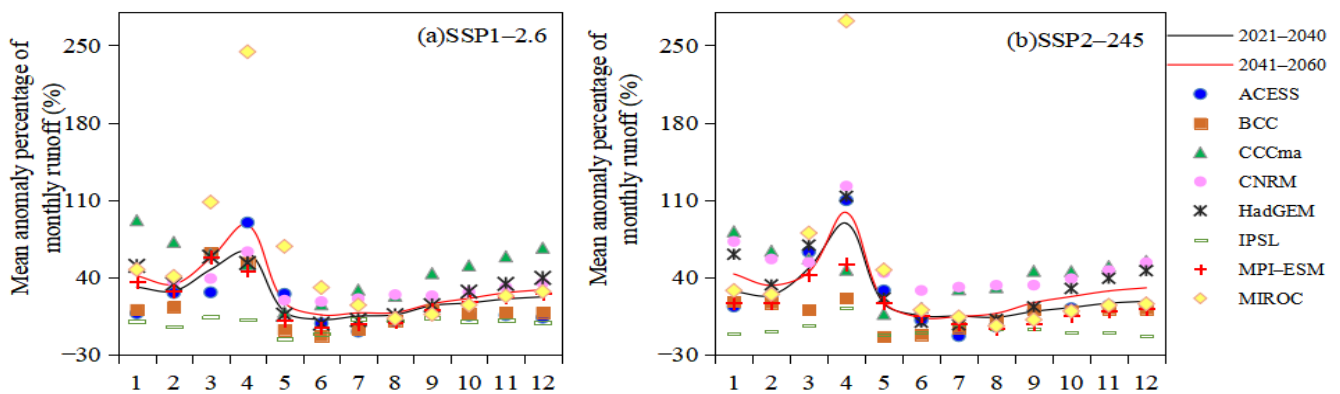
Figure 8. Projected changes (unit: %) in monthly runoff in the source region of the Yellow River Basin for 2021–2060 relative to 1995–2014 under (**a**) the SSP1–2.6 scenario and (**b**) the SSP2–4.5 scenario.

Figure 9 shows the changes in proportional monthly runoff of the annual total for 2021–2060 and for the first half and second half of the period under the SSP1–2.6 and SSP2–4.5 scenarios. Matching the changes in monthly runoff, the proportion of runoff was projected to increase by 0.1–1.0% from January to May and from September to December for both periods under both scenarios but was projected to decrease by 0.9–1.1% and by 0.7–1.2% from June to August for most GCMs under the SSP1–2.6 scenario and the SSP2–4.5 scenario, respectively.
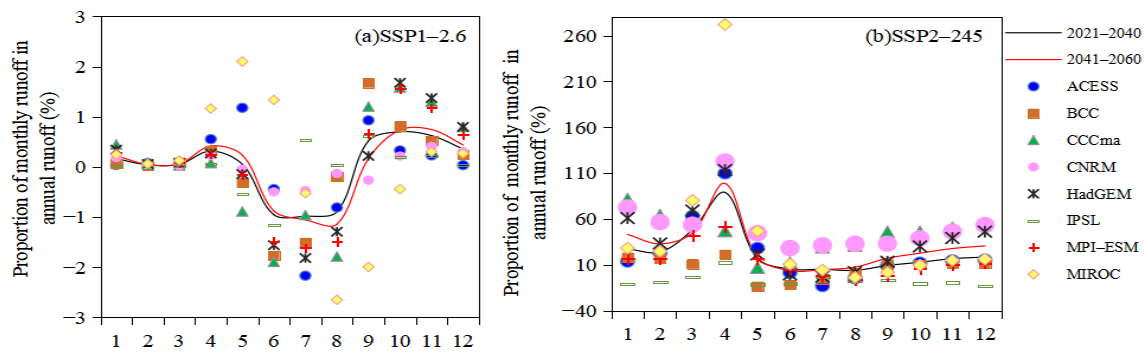
Figure 9. Projected changes (unit: %) in the percentage of monthly runoff to annual runoff for the source region of the Yellow River Basin for 2021–2060 relative to 1995–2014 under (**a**) the SSP1–2.6 scenario and (**b**) the SSP2–4.5 scenario.

In conclusion, the seasonal distribution of runoff was projected to be flatter in the source region of the Yellow River from 2021–2060, which would likely alleviate water scarcity in the dry and water storage seasons to some degree.

3.6. Variation in Extreme Runoff

Figure 10 shows the changes in extreme monthly high flow and low flow for 2021–2060 under the two scenarios. Extremely high monthly flow was expected to increase by 3.5–12.7% in the flood season and by 13.3–13.4% in the water storage season under both scenarios, whereas the extreme high flow in the dry season decreased by 2.3–23.1% under the two scenarios. Extremely low flow was projected to increase by 19.4–26.2% from February–April but to decrease by 5.0–8.9% in January, May, and December. This suggests that global warming will increase the flood risk in the flood and water storage seasons and increase the drought risk in January, May, and December, while a reduced drought risk will still exist in the dry season.
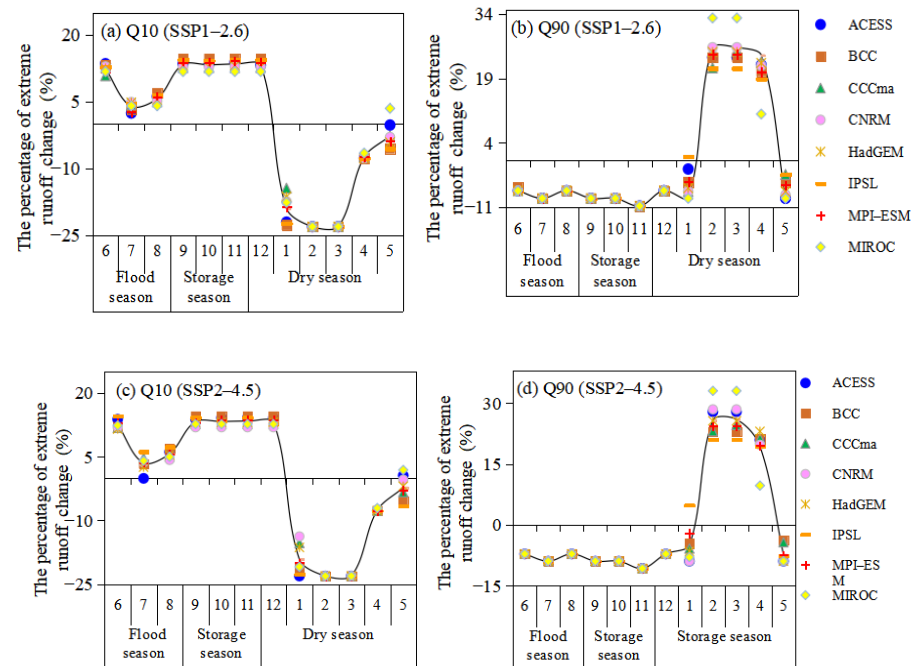
Figure 10. Projected changes (unit: %) in the ensemble mean Q10 and Q90 in the source region of the Yellow River Basin for 2021–2060 relative to 1995–2014 under (**a,b**) the SSP1–2.6 scenario and (**c,d**) SSP2–4.5 scenario.

4. Discussion

4.1. Hydrological Responses to Climate Change

The projection of water inflow and extreme hydrological events is important for the water resource security in the source region of the Yellow River Basin and even for the entire basin. A trend of a warmer and wetter climate and an increasing trend of annual runoff were projected in the study area for 2021–2060 under the SSP1–2.6 and SSP2–4.5 scenarios. The warming trend found in this study coincides with the warming for 2020–2059 relative to 1976–2015 under the scenarios of RCP 2.6, 4.5, and 8.5 based on eight CMIP5 GCMs. The wetter trend for this region, also found in this study, coincides with the trend found in this region under RCP 2.6, 4.5, and 8.5 based on CMIP5 GCMs [14] and the findings based on 12 CMIP6 GCMs under the SSP1–2.6, SSP2–4.5, SSP3–7.0, and SSP5–8.5 scenarios [17]. The trend of increase in annual runoff found in this study is in accordance with some previous studies [18,34] but in contrast to the trend of decrease reported in another research [14]. In the study area, monthly runoff was projected to increase in most months, and to increase by a greater magnitude in March and April than in other months. This could be attributed to the expectation of more precipitation and more meltwater under the condition of global warming [35], because glaciers and frozen soil cover parts of the study area. It is even indicated that thawing permafrost will inevitably release large volumes of water that could recharge surface and underground runoff in the dry season, and that advancement of the snowmelt period will change the schedule of runoff recharge in spring [36–39]. Conversely, rising temperatures will cause the increase in evapotranspiration that will consequently reduce runoff. The mechanism of melting of glaciers and frozen soil and the attribution of runoff change could be important topics for further study. Additionally, continued implementation of ecological protection projects will substantially increase the vegetation coverage in the study region, which could effectively change the runoff and have a long-term impact. The future changes in runoff caused by these factors should be further investigated and considered in regional developments in the source region of the Yellow River Basin.

4.2. Uncertainties of Projections

The degree of variation in the projected temperature and precipitation differed among the eight GCMs and between the two scenarios. Larger uncertainties in both the magnitude and the direction of change in runoff were projected because of the nonlinear responses of runoff to climate change. Interestingly, the opposite change in summer was projected in a previous study [40], which reported that runoff was expected to diminish from 2011–2050 relative to 1971–2010 under the RCP 2.6, 4.5, and 8.5 scenarios based on the VIC hydrological model and CMIP5 GCMs. Additionally, the study also projected more severe droughts from February–April but less severe droughts in January, May, and December. This conclusion is somewhat different from that of a previous study [41], which indicated that reductions in the duration and intensity of meteorological drought were expected in the source area of the Yellow River using an ensemble of CMIP5 GCMs and the Palmer drought severity index. Differences in the structure of GCMs, ensemble members of multiple GCMs, base periods, data used for model initial conditions, and downscaling methods can produce different results.

It is indicated that the uncertainties in the projections of runoff originate from each link in the simulation chain, including the selected SSP–RCP scenarios, GCMs, downscaling methods, hydrological models, and model parameterization [42–44]. In this study, the uncertainties related to the structure of GCMs and the emission scenarios were investigated by considering eight GCMs and two SSP–RCP scenarios. Furthermore, the MEMs of the eight selected GCMs were calculated to reduce the uncertainties of the projected variables, and recent research has demonstrated that different weighting sets of multiple models might improve the simulation performance, which is a subject that should be further explored [45]. Additionally, the SWAT model can simulate seasonal patterns of runoff. Therefore, projections based on the SWAT model have the potential for providing water resource managers

and policymakers with valuable information. However, it remains important to explore the uncertainties associated with the downscaling method, hydrological structure, and parameters used in the simulations. Uncertainty attribution is an interesting topic that has been explored in a previous study [46] and is worth discussing further concerning different regions.

However, high flows were underestimated by the SWAT model in this study. This suggests that there is space to improve the parametrization of SWAT in the study area. Previous research also showed that high monthly flows through the Tangnaihai station were either underestimated or overestimated to some degree in different years by the SWAT model [47,48], while floods through the station were underestimated by the SWAT model [46]. Although bias and uncertainties exist, SWAT model is still a popular tool to investigate the hydrological response to climate change as well as land cover change historically or in the future, (e.g., [25,27,33,45,48]).

5. Conclusions

Water resource availability and hydrological disaster risk, which are the key issues in the source region of the Yellow River Basin, have already been and will continue to be affected by climate change. This study projected the impact of climate change on runoff in the source region of the Yellow River Basin with the goal of achieving carbon neutrality.

The climate is projected to become warmer and wetter from 2021–2060 under both the SSP1–2.6 scenario and the SSP2–4.5 scenario. The MEM of annual air temperature is projected to rise by 1.3–1.6 °C, and annual precipitation is projected to increase by 11.1–11.2%. However, the magnitude of the projected increase varies among the eight CMIP6 GCMs and between the two scenarios considered in this study. The largest increase in annual temperature is projected to be 2.2 and 2.6 °C by the CCCma model under the SSP1–2.6 scenario and the SSP2–4.5 scenario, respectively, and the smallest increase is projected to be 0.8 °C by the BCC and MPI–ESM models under the SSP1–2.6 scenario and by the MPI–ESM model under the SSP2–4.5 scenario. The largest increase in annual precipitation is projected to be 25.5% by the CNRM model. However, the increase in annual precipitation is projected to be less than 15.0% for most models.

The amount of annual runoff is expected to increase and the seasonal pattern of runoff is projected to change. The MEM of annual runoff is expected to increase by 12.6% and 11.8% under the SP1–2.6 scenario and SSP2–4.5 scenario, respectively. However, notable decadal fluctuation is projected. The largest increasing magnitudes will be up to 14.1–15.2% in the 2040s and the 2050s. Under the background of annual runoff increase, the seasonal pattern is projected to change slightly. The proportion of runoff is generally projected to decrease in the flood season and increase in the dry season, especially under the SSP1–2.6 scenario. Such changes would alleviate water stress in the source region of the Yellow River to some degree.

The projections also indicate a higher risk of flooding in the flood and water storage seasons but a higher risk of drought in January, May, and December. Extremely high monthly flow is projected to increase by 3.5–13.4% in the flood and water storage seasons, and extreme low flow is projected to increase by 19.4–26.2% from February–April but to decrease in January, May, and November. However, water resource managers should be cautious when using the projected changes in flooding based on Q10 because of the underestimation of extremely high monthly flow.

In conclusion, the source region of the Yellow River Basin will experience a warmer and wetter climate in the coming 40 years. Water availability will increase in all months. There will be a higher risk of flooding in the flood season but a lower risk of drought from February to April. Generally, the flatter pattern of runoff would likely alleviate water scarcity in the dry and the water storage seasons to some degree, and the increase in monthly runoff in water storage season will benefit hydroelectric power generation and agriculture and animal husbandry production. However, in some years, the increase in

Q10 in the flood season will likely increase flood prevention pressure, and the decrease in Q90 in May will likely obstruct grass revival.

Author Contributions: Conceptualization, Y.L.; Data curation: H.L. and J.Y.; Formal analysis, Y.L., B.Z.; Methodology, Y.L.; Resources, L.L. (Lin Li), H.X. and L.L. (Lyuliu Liu); Supervision, L.L. (Lyuliu Liu); Writing—original draft, Y.L.; Writing—review and editing, Y.L., L.L. (Lyuliu Liu), H.L., S.T. All authors have read and agreed to the published version of the manuscript.

Data Availability Statement: Details of all data generated or analyzed during this study are included in the published article.

Conflicts of Interest: The authors declare no conflict of interest.

References

1. Yang, C.H.; Wang, Y.J.; Su, B.D.; Pu, Y.; Wang, Y.; Jiang, T. Runoff variation trend of Ganjiang River basin under the goal of "Double Carbon" in China. *Clim. Chang. Res.* **2022**, *18*, 177–218. (In Chinese)
2. Chen, Y. A re–analysis of the concept of carbon neutrality. *China Popul. Resour. Environ.* **2022**, *32*, 1–12.
3. Jing, T.; Guo, S.; Deng, L.; Yin, J.; Pan, Z.; He, S.; Li, Q. Adaptive optimal allocation of water resources response to future water availability and water demand in the Han River basin, China. *Sci. Rep.* **2021**, *11*, 7879.
4. Liu, Y.H.; Li, H.M.; Li, L.; Wang, Q.C.; Xu, X.H. Comparative analysis of three models to the study on risk precipitation threshold value in Datong river basin. *Hubei Agric. Sci.* **2021**, *60*, 27–31. (In Chinese)
5. Jiang, T.; Lü, Y.R.; Huang, J.L.; Wang, Y.J.; Su, B.D.; Tao, H. New scenarios of CMIP6 model (SSP–RCP) and its application in the Huaihe River Basin. *Adv. Meteorol. Sci. Technol.* **2020**, *10*, 102–109. (In Chinese)
6. Liu, L.; Xiao, C.; Liu, Y. Projected Water Scarcity and Hydrological Extremes in the Yellow River Basin in the 21st Century under SSP–RCP Scenarios. *Water* **2023**, *15*, 446. [CrossRef]
7. Li, L.; Shen, H.Y.; Dai, S.; Xiao, J.S.; Shi, X.H. Response to Climate Change and Prediction of Runoff in the Source Region of Yellow River. *Acta Geogr. Sin.* **2011**, *66*, 1261–1269. (In Chinese)
8. Zhang, X.; Liu, L. Study on the change characteristics of water resources in the Yellow River Basin from 1998 to 2018. *Ground Water* **2020**, *42*, 187–291. (In Chinese)
9. Haichao, Y.; Zhang, Y.; Jingzhu, M.; Jiabing, G.; Peiyuan, C. Variation of observed and natural runoff of Yellow River from 1969 to 2018. *Bull. Soil Water Conserv.* **2020**, *40*, 1–7.
10. Liu, X.; Liu, Y.; Zhao, J.; Zhao, Y.; Li, J. Analysis of the variable characteristics of water resources in the Main Stream of Yellow river since 1998. *Yellow River* **2019**, *41*, 70–75. (In Chinese)
11. Wang, H.; Li, D. Research progress on variations and effector of the runoff in the source region of the Yellow River. *Plateau Mt. Meteorol. Res.* **2013**, *33*, 93–97. (In Chinese)
12. Hou, B.; Jiang, C.; Sun, O.J. Differential changes in precipitation and runoff discharge during 1958–2017 in the headwater region of Yellow River of China. *J. Geogr. Sci.* **2020**, *30*, 1401–1418. [CrossRef]
13. Zhang, L.X.; Chen, X.L.; Xin, X.G. Short commentary on CMIP6 Scenario Model Intercomparison Project (Scenario MIP). *Clim. Chang. Res.* **2019**, *15*, 519–525. (In Chinese)
14. Hu, J.; Wu, Y.; Sun, P.; Zhao, F.; Jin, Z. Predicting long–term hydrological change caused by climate shifting in the 21st century in the headwater area of the Yellow River Basin. *Stoch. Environ. Res. Risk Assess.* **2022**, *36*, 1651–1668. [CrossRef]
15. Xin, X.; Wu, T.; Zhang, J.; Yao, J.; Fang, Y. Comparison of CMIP6 and CMIP5 simulations of precipitation in China and the East Asian summer monsoon. *Int. J. Climatol.* **2020**, *40*, 6423–6440. [CrossRef]
16. Hu, Y.Y.; Xu, Y.; Li, J.J.; Han, Z.Y. Evaluation on the performance of CMIP6 global climate models with different horizontal resolution in simulating the precipitation over China. *Clim. Chang. Res.* **2021**, *17*, 1–19. (In Chinese)
17. Sun, Z.; Liu, Y.; Zhang, J.; Chen, H.; Shu, Z.; Chen, X.; Jin, J.; Guan, T.; Liu, G.; He, R.; et al. Projecting future precipitation in the Yellow River basin based on CMIP6 models. *J. Appl. Meteorol. Climatol.* **2022**, *61*, 1399–1417. [CrossRef]
18. Jia, H.J.; Li, X.H.; Wen, J.; Chen, Y.L. Runoff change simulation and future trend projection in the source area of the Yellow River. *Resour. Sci.* **2022**, *44*, 1292–1304. [CrossRef]
19. Xu, Y.; Gao, X.J.; Shen, Y.; Xu, C.H.; Shi, Y.; Giorgi, F. A daily temperature dataset over China and its application in validating a RCM simulation. *Adv. Atmos. Sci.* **2009**, *26*, 763–772. [CrossRef]
20. Wu, J.; Gao, X. A grid daily observation data set over China region and comparison with the other datasets. *Chin. J. Geophys.* **2013**, *56*, 1102–1111. (In Chinese)

21. Wei, L.; Liu, L.; Jiang, C.; Wu, Y.; Xin, X.; Yang, B.; Tang, H.; Li, Y.; Wang, Y.; Zhang, T.; et al. Simulation and Projection of Climate Extremes in China by a Set of Statistical Downscaled Data. *Int. Environ. Res. Public Health* **2022**, *19*, 6398. [CrossRef] [PubMed]

22. Liu, L.; Wei, L.; Xu, Y.; Xin, X.; Xiao, C. Projection of climate change impacts on ecological flow in the Yellow River basin. *Adv. Water Sci.* **2021**, *32*, 824–833. (In Chinese)

23. Bai, S.; Wang, L.; Shi, J.; Li, W. Runoff simulation for Kaidu river basin based on SWAT model. *J. Arid. Land Resour. Environ.* **2013**, *27*, 79–84. (In Chinese) [CrossRef]

24. Si, J.; Li, J.; Yang, Y.; Qi, X.; Li, J.; Liu, Z.; Li, M.; Lu, S.; Qi, Y.; Jin, C. Evaluation and Prediction of Groundwater Quality in the Source Region of the Yellow River. *Water* **2022**, *14*, 3946. [CrossRef]

25. Ji, G.; Lai, Z.; Xia, H.; Liu, H.; Wang, Z. Future runoff variation and flood disaster prediction of the Yellow River Basin based on CA–Markov and SWAT. *Land* **2021**, *10*, 421. [CrossRef]

26. Arnold, J.G.; Srinivasan, R.; Muttiah, R.S. Large area hydrologic modeling and assessment part I: Model development. *J. Am. Water Resour. Assoc.* **1998**, *34*, 73–89. [CrossRef]

27. Wu, J.; Zheng, H.; Xi, Y. Swat–based runoff simulation and runoff responses to climate change in the Headwaters of the Yellow River, China. *Atmosphere* **2019**, *10*, 509. [CrossRef]

28. Moriasi, D.N.; Gitau, M.W.; Pai, N.; Daggupati, P. Hydrologic and water quality models: Performance measure and evaluation criteria. *Trans. Am. Soc. Agric. Biol. Eng.* **2015**, *58*, 1763–1785.

29. Beven, K.L. *Rainfall–Runoff Modeling: The Primer*; John Wiley & Sons: New York, NY, USA, 2000.

30. Wang, S.; Hongmei, X.; Lyuliu, L.; Yong, W.; Awei, S. Projection of the impacts of Global warming of 1.5°Cand 2°Con runoff in the upper–Middle reaches of Huaihe river basin, Journal of natural resources. *J. Nat. Resour.* **2018**, *33*, 1966–1978. (In Chinese)

31. Pandi, D.; Kothandaraman, S.; Kuppusamy, M. Simulation of water balance components using SWAT model at sub catchment level. *Sustainability* **2023**, *15*, 1438. [CrossRef]

32. Qin, P.; Liu, M.; Du, L.; Xu, H.; Liu, K.; Xiao, C. Climate change impacts on runoff in the upper Yangtze River basin. *Clim. Chang. Res.* **2019**, *15*, 405–415. (In Chinese)

33. Wang, Y.; Xu, H.M.; Li, Y.H.; Liu, L.L.; Hu, Z.H.; Xiao, C.; Yang, T.T. Climate change impacts on runoff in the Fujiang River Basin based on CMIP6 and SWAT Model. *Water* **2022**, *14*, 3614. [CrossRef]

34. Wei, J.; Chang, J.; Chen, L. Runoff change in upper reach of Yellow River under future climate change based on VIC model. *J. Hydroelectr. Eng.* **2016**, *35*, 65–74. (In Chinese)

35. Hamlet, A.F.; Byun, K.; Robeson, S.M.; Widhalm, M.; Baldwin, M. Impacts of climate change on the state of Indiana: Ensemble future projections based on statistical downscaling. *Clim. Chang.* **2020**, *163*, 1881–1895. [CrossRef]

36. Ding, Y.; Zhang, S.; Wu, J.; Zhao, Q.; Li, X.; Qin, J. Recent progress on studies on cryospheric hydrological processes changes in China. *Adv. Water Sci.* **2020**, *31*, 690–702.

37. Zhang, F.; Liu, J.; Gong, T. Winter runoff in a typical Alpine permafrost region, Tibet–Himalayas. *Adv. Earth Sci.* **2006**, *21*, 1334–1338.

38. Zhang, T.; Li, D.; Lu, X. Response of runoff components to climate change in the source region of the Yellow River on the Tibetan plateau. *Hydrol. Process.* **2022**, *36*, e14633. [CrossRef]

39. Qin, Y.; Yang, D.; Gao, B.; Wang, T.; Chen, J.; Chen, Y.; Zheng, G. Impacts of climate warming on the frozen ground and eco-hydrology in the Yellow River source region. *China Sci. Total Environ.* **2017**, *605–606*, 830–841. [CrossRef]

40. Shao, Y.; Dong, Z.; Meng, J.; Wu, S.; Li, Y.; Zhu, S.; Zhang, Q.; Zheng, Z. Analysis of Runoff Variation and Future Trends in a Changing Environment: Case Study for Shiyanghe River Basin, Northwest China. *Sustainability* **2023**, *15*, 2173. [CrossRef]

41. Zhang, L.; Zheng, W.; Yang, X.; Wang, Y.; Zhang, M.; Yu, X. Temporal–spatial characteristics of drought in source region of Yellow River based on CMIP5 multi–mode ensemble and PDSI. *Water Resour. Prot.* **2019**, *35*, 95–99. (In Chinese)

42. Liu, L.; Fischer, T.; Jiang, T.; Luo, Y. Comparison of uncertainties in projected flood frequency of the Zhujiang River, South China. *Quat. Int.* **2013**, *304*, 51–61. [CrossRef]

43. Kundzewicz, Z.W.; Krysanova, V.; Dankers, R.; Hirabayashi, Y.; Kanae, S.; Hattermann FF Huang, S.; Milly PC, D.; Stoffel, M.; Driessen, P.P.J.; Matczak, P.; et al. Differences in flood hazard projections in Europe–their causes and consequences for decision making. *Hydrol. Sci. J.* **2020**, *62*, 1–14. [CrossRef]

44. Huang, S.; Shah, H.; Zaz, B.S.; Shrestha Narayan Mishra, V.; Daggupati, P.; Ghimire, U.; Vetter, T. Impacts of hydrological model calibration on projected hydrological changes under climate change–a multi–model assessment in three large river basins. *Clim. Chang.* **2020**, *163*, 143–1164. [CrossRef]

45. Hattermann, F.F.; Vetter, T.; Breuer, L.; Su BDaggupati, P.; Donnelly, C.; Fekete, B.; Flörke, F.; Gosling, S.N.; Hoffmann, P.; Liersch, S.; et al. Sources of uncertainty in hydrological climate impact assessment: A cross–scale study. *Environ. Res. Lett.* **2018**, *13*, 015006. [CrossRef]

46. Huang, S.; Kumar, R.; Flörke, M.; Yang, T.; Hundecha, Y.; Kraft, P.; Gao, C.; Gelfan, A.; Liersch, S.; Lobanova, A.; et al. Evaluation of an ensemble of regional hydrological models in 12 large–scale river basins worldwide. *Clim. Chang.* **2017**, *141*, 381–397. [CrossRef]

47. Liu, C.; Li, D.; Tian, Y.; Hao, F.; Yang, G. An application study of DEM based distributed hydrological model on macroscale watershed. *Prog. Geogr.* **2003**, *22*, 437–445. (In Chinese)
48. Chen, L.; Liu, C. Influence of climate and land–cover change on runoff of the source regions of the Yellow River. *China Environ. Sci.* **2007**, *27*, 559–565. (In Chinese)